ADVANCED ENGINEERING MATERIALS

DOI: 10.1002/adem.201000091

Bi-Stable Adhesion of a Surface with a Dimple

By *Robert M. McMeeking*, Lifeng Ma* and *Eduard Arzt*

In this paper, we propose a new adhesive system of dimpled surfaces. The principle is derived from a contact mechanics model. The material is assumed to be linear elastic and isotropic, and attraction between the surfaces of the half-spaces is modeled via the concept of a specific adhesion energy. It is found that large and small detachments are unstable and will either grow or shrink spontaneously when their sizes are perturbed. It is shown that this phenomenon can lead to a new bi-stable adhesive system in which weak adhesion can be converted to strong adhesion by the application of pressure.

Adhesion due to molecular interactions such as van der Waals forces is of great importance for many technological and biological systems.[1] In regard to such adhesion, innovative patterned surfaces are currently causing a change of paradigm, and are creating new opportunities for sticky devices. Examples are gecko-like fibrillar surfaces (for a review see[2]), and devices with microfluidic channels.[3] In these cases, detachment is inhibited by the heterogeneous nature of the adhered structures, enhancing the energy dissipated even in cases where the adhering area is a fraction of the total available surface. Within this context, we propose in the current paper a new adhesive system characterized by arrangements of dimples on one or both surfaces. We also note that the present paper demonstrates that useful developments in new materials can originate from theoretical modeling.

When bodies interacting with each other adhere at non-planar surfaces, elasticity plays an important role in determining the adhesive and repulsive interactions. Examples include the case of a sphere adhering to a half-space, as modeled by Johnson, Kendall, and Roberts (JKR),[4] where there is elastic flattening of the sphere and elastic indentation of the half-space. In the JKR problem, adhesion is modeled through an energy balance involving changes of surface and elastic energy, with details of the interaction at a distance neglected. This aspect of the behavior was relaxed by Maugis,[5] who augmented the JKR solution with a model having a constant traction when the bodies are closer than a critical distance. Further refinements of the Maugis[5] solution were provided by Kim *et al.*[6] The JKR solution for a single spherical protrusion has also been extended to multiple asperities, represented as periodic waviness, to model adhesion of rough surfaces.[7–10]

An equivalent problem is adhesion of a flat surface to another one having a dimple (Fig. 1). As half-spaces are brought toward each other, the surfaces far away from the dimple will adhere to each other first, and the attached area will grow progressively. Completion of the adhesion will be resisted by the elastic distortion necessary for the flat surface to be pulled into the dimple. If the dimple is deep, the materials are stiff or the adhesion is weak, it will be difficult for the attraction of adhesion to eliminate detached regions, unless significant compression is applied. Conversely, if the dimple is shallow, the materials are compliant, or the adhesion is strong, complete adhesion may be achieved spontaneously without the application of compression, unless trapped air

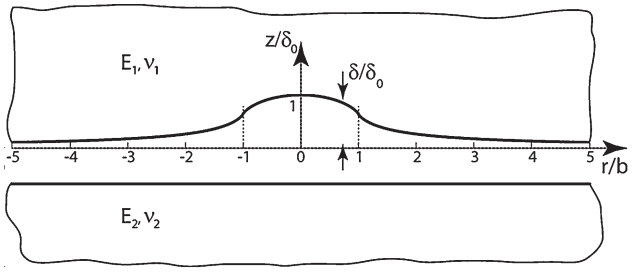

Fig. 1. Two isotropic, linear elastic half-spaces, one with a flat surface and the other having a dimple with effective radius b and depth δ_0. The upper half-space has Young's modulus E_1 and Poisson's ratio ν_1, whereas the lower half-space has properties E_2 and ν_2.

[*] *Prof. R. M. McMeeking, Prof. E. Arzt*
INM – Leibniz Institute for New Materials, Modeling and Simulation Group Campus D2 2, 66123 Saarbruecken, Germany
E-mail: rmcm@engineering.ucsb.edu
Prof. R. M. McMeeking
Department of Mechanical Engineering and Materials, University of California Santa Barbara, California 93106, USA
Prof. E. Arzt
INM – Leibniz Institute for New Materials, Functional Surfaces Group, and Saarland University
Campus D2 2, 66123 Saarbruecken, Germany
Dr. L. Ma
MOE Key Laboratory for Strength and Vibration, Xi'an Jiaotong University Xi'an 710049, China

COMMUNICATION

resists the tendency for spontaneous closure of the detachment.[7,8] Analysis of this problem, without regard to trapped air, is undertaken below. The outcome bears some similarity to results presented for adhesion involving periodically wavy surfaces.[7–10] Due to its simplicity, the problem of a single dimple on an otherwise featureless surface furnishes some insights otherwise not readily available.

Model

Consider the undistorted shapes of a half-space with a flat surface and a half-space with a dimple in its surface as shown in Figure 1. The shape of the dimple has been chosen for ease of analysis, but its characteristics are representative of any that is isolated. The dimple is axisymmetric with a shape given by

$$\delta = \frac{2}{\pi}\delta_0 \varepsilon\left(\frac{r}{b}\right) \qquad \frac{r}{b} \le 1 \tag{1a}$$

$$\delta = \frac{2r}{\pi b}\delta_0 \left[\varepsilon\left(\frac{b}{r}\right) - \left(1 - \frac{b^2}{r^2}\right)\kappa\left(\frac{b}{r}\right)\right] \qquad \frac{r}{b} \ge 1 \tag{1b}$$

where δ_0 is the maximum depth of the dimple, $\varepsilon(\theta)$ the complete elliptic integral of the second kind of its argument θ, and $\kappa(\theta)$ is the complete elliptic integral of the first kind of its argument θ.

When they are brought into contact, the surfaces of the half-spaces adhere to each other such that the reduction of potential energy per unit adhered area is given by

$$w_0 = \gamma_1 + \gamma_2 - \gamma_{12} \tag{2}$$

where γ_1 and γ_2 are the surface energies of the upper and lower half-space, and γ_{12} is the energy of the interface between the half-spaces in contact.

The half-spaces are linear elastic and isotropic, with Young's moduli E_1 and E_2 and Poisson's ratios ν_1 and ν_2. The dimple is considered to be shallow (i.e., $\delta_0 << b$), so that elastic distortions caused by tractions applied to the surface of the half-space containing the dimple can be computed as the displacements of a half-space having a flat surface. As noted by Johnson,[11] when a uniform pressure p is applied around the origin to a circular region of radius b on the surface of a half-space with a flat surface, the surface displacements in the z direction are given by Equation (1a and b) with δ_0 replaced by $2pb/E'$, where the resulting displacements are in the same direction as the normal pressure p, and $E' = E/(1-\nu^2)$. It then follows that the shape of the surface of the upper half-space can be made to be identical to the shape of the lower one when both are subject to a tensile traction T on their surfaces within the region at the origin having radius b, where

$$T = \frac{\delta_0 E^*}{2b} \tag{3}$$

with E^* the combined modulus, given by

$$\frac{1}{E^*} = \frac{1-\nu_1^2}{E_1} + \frac{1-\nu_2^2}{E_2} \tag{4}$$

When the two surfaces are completely adhered to each other with no detached area, and a uniform tensile traction is applied, as depicted in Figure 2, there is a stress at the interface given by

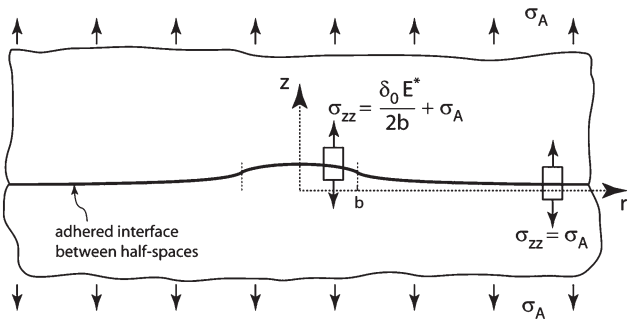

Fig. 2. The two half-spaces adhering completely to each other and under applied load. The tensile stress at the interface is indicated.

$$\sigma_{zz} = \sigma_A + \frac{\delta_0 E^*}{2b} \qquad \frac{r}{b} \le 1 \tag{5a}$$

$$\sigma_{zz} = \sigma_A \qquad \frac{r}{b} \ge 1 \tag{5b}$$

where σ_A is the applied tensile stress. Note that there are no shear tractions or shear stresses of any kind at the interface, so that the resulting stress state represents the case of frictionless adhesion. Note that the above solution is used by Gao and Yao,[12] but in a different context.

The Effect of a Detachment under Applied Load

Now introduce a detachment of radius a as shown in Figure 3. This feature will relax to zero the stresses of Equation (5) previously present at the interface within the region $r \le a$. Since these stresses are tensile, there will be a driving force, G, the energy release rate, for extending the detachment.[11] In Appendix I we compute G. The equilibrium requirement that G is equal to the adhesion energy w_0 provides the relationship between the detachment length and the applied stress as follows:

$$\sigma_A = E^*\left(\sqrt{\frac{\pi w_0}{2aE^*}} - \frac{\delta_0}{2b}\right) \qquad a \le b \tag{6a}$$

$$\sigma_A = E^*\left[\sqrt{\frac{\pi w_0}{2aE^*}} - \frac{\delta_0}{2b}\left(1 - \sqrt{1 - \frac{b^2}{a^2}}\right)\right] \qquad a > b \tag{6b}$$

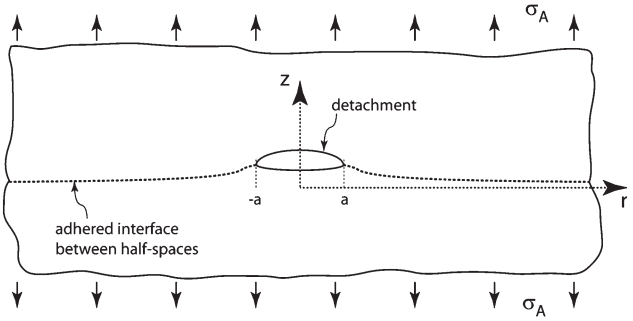

Fig. 3. The adhered half-spaces under applied load with a detachment of radius a at the interface.

ADVANCED ENGINEERING MATERIALS

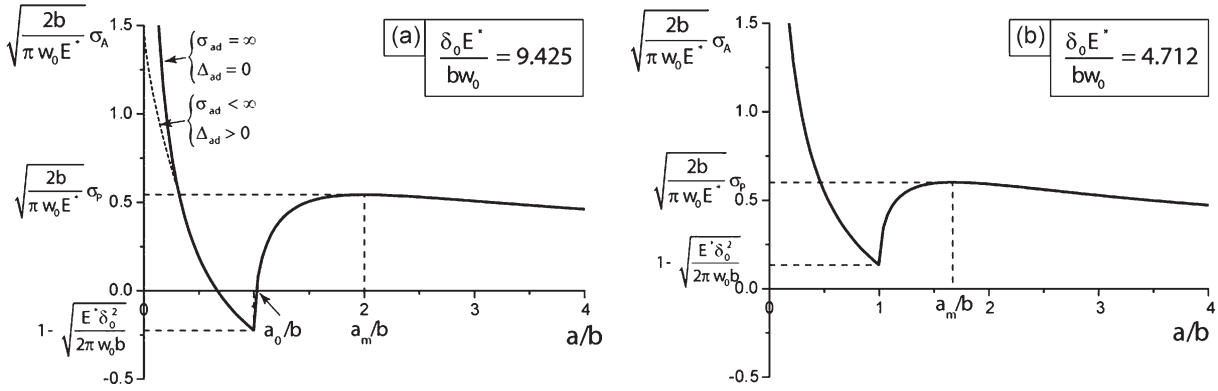

Fig. 4. Plots of the applied stress, σ_A, in equilibrium with a detachment of radius a for an adhesion energy w_0; (a) shows the relationship for a pair of surfaces with a relatively deep dimple, a relatively high effective elastic modulus, E^*, a relatively small dimple radius, and a relatively low adhesive energy; the dashed line shows our estimate of the behavior for a system with finite adhesive strength and interaction distance; (b) shows the relationship for a pair of surfaces with a relatively shallow dimple, a relatively low effective elastic modulus, a relatively large dimple radius, and a relatively high adhesive energy.

The result from Equation (6) giving $\sigma_A\sqrt{2b/\pi w_0 E^*}$ versus a/b is shown in Figure 4, where two cases are illustrated. In Figure 4(a), $\delta_0^2 E^*/bw_0 > 2\pi$ (a value of 9.425 has been chosen for clarity), and as a result, there is a region of the plot where the applied stress in equilibrium with the detachment is compressive (i.e., negative); this relationship is shown as the full line in Figure 4(a). In Figure 4(b), $\delta_0^2 E^*/bw_0 < 2\pi$ (a value of 4.712 has been chosen for clarity), and in this case the applied stress at equilibrium is always tensile (i.e., positive).

A detachment is stable if it maintains its current length and is unstable if it grows or shrinks spontaneously. In Appendix II we show that stability of the detachment is assured if $\partial\sigma_A/\partial a > 0$. As a consequence, stability in the equilibrium state occurs in the range $b < a < a_m$ (see Fig. 4), where a_m is the radius of the detachment at which the applied stress in equilibrium with it has a maximum. In the stable condition, a perturbation of the diameter of the detachment will be eliminated spontaneously; i.e., if the diameter is increased, the detachment will shrink back to its equilibrium size, and if the diameter is reduced, the detachment will grow back to its equilibrium size. The equilibrium configuration is unstable for values of a lying outside the range $b < a < a_m$. When an unstable, equilibrium detachment with its radius in this range is perturbed by having its length increased at constant applied load, it will spontaneously continue to lengthen; when it is perturbed by being made smaller, it will spontaneously continue to shrink.

Attachment and Detachment

Weak Adhesion, Stiff Materials, or a Shallow Dimple

Now consider adhesion between half-spaces having the interaction shown in Figure 4(a), i.e., $\delta_0^2 E^*/bw_0 > 2\pi$. As a starting point, assume that the surfaces are already adhered with a finite detachment radius but with no applied stress. Inspection of Figure 4(a) indicates that, for it to be in stable equilibrium, the detachment must have the radius a_0, whose value can be found by setting σ_A to zero in Equation (6b) and selecting the root $a_0 > b$. If a tensile stress is applied and gradually increased under load control, the detachment will grow stably at first, consistent with the graph of Figure 4(a). Such stable growth will continue until the radius a reaches the value a_m. Any attempt thereafter to increase the applied stress will lead to unstable propagation of the detachment, and the half-spaces will separate from each other. The radius, a_m, at which this pull-off will occur can be computed by obtaining $\partial\sigma_A/\partial a$ from Equation (6b) and setting it to zero (see Appendix II). The result for a_m,

$$\frac{a_m}{b} = \left[\frac{E^*\delta_0^2}{\pi w_0 b} + \sqrt{\left(\frac{E^*\delta_0^2}{\pi w_0 b}\right)^2 - \frac{1}{27}}\right]^{\frac{1}{3}} + \left[\frac{E^*\delta_0^2}{\pi w_0 b} - \sqrt{\left(\frac{E^*\delta_0^2}{\pi w_0 b}\right)^2 - \frac{1}{27}}\right]^{\frac{1}{3}} \tag{7}$$

is plotted in Figure 5 versus $w_0 b/E^*\delta_0^2$. The consequent stress at pull-off, σ_P, obtained by inserting a_m in place of a in Equation (6b), is plotted also against $w_0 b/E^*\delta_0^2$ in Figure 5. It should be

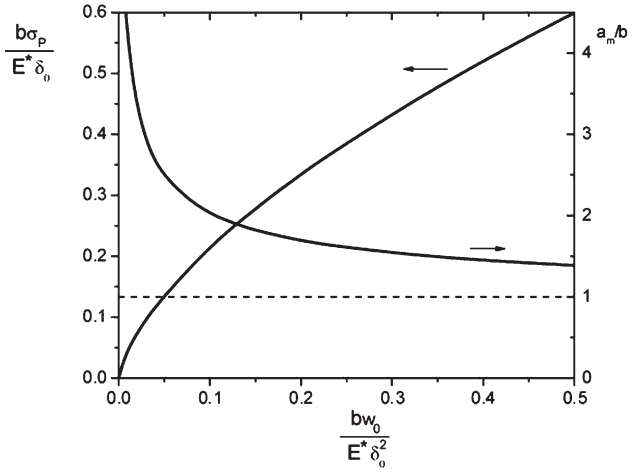

Fig. 5. Graphs of the pull-off stress, σ_P, as a function of $bw_0/E^*\delta_0^2$, and the detachment radius, a_m, at which pull-off occurs.

noted that even if the applied stress is reduced once the condition $a > a_m$ is reached to try to keep the system in equilibrium [i.e., in an attempt to keep the applied stress at its equilibrium value as shown in Figure 4(a)], the detachment will continue to grow since the equilibrium state in this regime is unstable; any small perturbation of the system, whether thermal, acoustic, or due to instrumental imprecision, will induce detachment growth.

Now return to the original configuration with a stable detachment of radius a_0 at zero applied stress. Let a compressive stress be applied, with a gradually increasing magnitude. The curve in Figure 4(a) indicates that in this situation, the detachment will diminish in radius, doing so stably until it reaches b. At this stage, the configuration becomes unstable, since $\partial\sigma_A/\partial a < 0$ for perturbations of a that take it below b. As a consequence, the detachment radius will reduce in an unstable manner, until it disappears. Thus, complete adhesion in a vacuum can be achieved if sufficient compressive stress is applied. In analogy to the situation with pull-off, the unstable disappearance of the detachment cannot be halted by an attempt to increase the applied stress to keep the system in equilibrium. Once the attachment process commences with a reducing below b, the system is in an unstable state even if the stress is in equilibrium with the radius of the detachment consistent with Figure 4(a). In the presence of trapped air, the increase in pressure as the detachment closes will inhibit such closure, eventually terminating it. This situation, for multiple detachments within periodically wavy surfaces, has been commented upon by Johnson[7] and analyzed by Hui *et al*.[8]

Note that since $\delta_0^2 E^*/bw_0 > 2\pi$, the phenomena we have just described are associated with a relatively deep dimple both absolutely and relative to its diameter, a pair of relatively stiff materials and weak adhesion between the half-spaces. For these reasons, the dimple presents some resistance to the processes needed to achieve complete adhesion, because of the significant elastic strain energy required to distort material into the dimple. This strong resistance is not compensated for adequately by the modest adhesive energy. As a consequence, this case exhibits bi-stable adhesion, at least in a vacuum or in a situation where there is a vent, so that air trapped in the dimple can escape. That is, a stable detachment of radius a_0 can exist at zero applied load, in which case the two surfaces may be separated relatively easily by the application of tension. However, if compression is applied to the system, the detachment can be eliminated completely, and we can expect this configuration to be difficult to pull apart. This latter point is explored in the next paragraph.

Staying with the same condition, $\delta_0^2 E*/bw_0 > 2\pi$, we now consider the configuration in which the two half-spaces are adhered completely, with no detachment present, i.e., $a = 0$. To detach the half-spaces from each other, one would apply a tensile stress, which is predicted to be infinite.[4,5] To overcome this difficulty, Johnson[7] postulated the presence of small initial detachments in an otherwise completely attached adhesion. An alternative remedy is the introduction of a more realistic model for the adhesive interactions, such as van der Waals phenomena.[1] Failing that, a simpler, but credible approach is the use of a Dugdale style interaction, or cohesive (i.e., adhesive) zone, as introduced into the adhesion literature by Maugis,[5] in which the surfaces of the half spaces attract each other with a constant tension, σ_{ad}, in those regions where they are closer to each other than a critical distance, Δ_{ad}. The product $\sigma_{ad}\Delta_{ad}$ equals w_0.[5] In their work, Hui *et al*.[8] utilized such a Dugdale style cohesive zone, and Carbone and Mangialardi[9] adopted a variant. Let us assume that a Dugdale style cohesive zone is appropriate for our problem, and consider a gradually increasing tensile stress, σ_A, applied to the completely adhered pair of half-spaces, so that within the dimple, the stress at the interface is given by Equation (5a). The half-spaces will remain adhered to each other without any detachment until the stress in Equation (5a) is equal to σ_{ad}, i.e., until

$$\sigma_A = \sigma_{ad} - \frac{\delta_0 E^*}{2b} \tag{8}$$

At this stage an incipient detachment will develop, but at first the separating surfaces within it will continue to attract each other with a tensile stress σ_{ad} between them. Since Equation (8) implies that the tensile stress across the interface everywhere within $r \le b$ is equal to σ_{ad}, we assume that this entire region begins to separate when the applied stress reaches the level given by Equation (8). Furthermore, the region that is detaching will immediately spread beyond b because the Dugdale model requires the stress intensity factor to be equal to zero so that there is no singularity in the stress. The stress intensity factor is now given by[13]

$$K_I = \frac{2}{\pi}\left[\sigma_A + \frac{\delta_0 E^*}{2b}\left(1 - \sqrt{1 - \frac{b^2}{c^2}}\right) - \sigma_{ad}\right]\sqrt{\pi c} \tag{9}$$

where c is the radius of the circle that is experiencing detachment (while still feeling mutual attraction). Since the stress intensity factor has to be zero, the relationship between c and the applied stress from Equation (9) is

$$c = \frac{b}{\sqrt{1 - \left[\dfrac{\sigma_A - \left(\sigma_{ad} - \frac{\delta_0 E^*}{2b}\right)}{\frac{\delta_0 E^*}{2b}}\right]^2}} \tag{10}$$

so that as the applied stress rises above $\sigma_{ad} - \delta_0 E^*/2b$, this radius increases beyond a in a stable manner.

This process will continue as given by Equation (10) until the distance across the gap in the center of the detachment reaches Δ_{ad}. Thereafter, a zone without adhesive interaction will develop in the center of the detachment, i.e., the radius, a, of the traction free zone becomes non-zero and grows, and the stress intensity factor is no longer given by Equation (9). Further calculations illustrating this point are beyond the scope of the current paper. However, we can

sketch out the following scenario. We infer that the system becomes unstable as soon as the traction free zone appears. In the absence of a proper analysis of the axisymmetric situation, we conclude that instability will set in from consideration of an assessment of the equivalent plane strain problem that is summarized in Appendix III. Consequently, as a increases from zero, the applied stress will fall while the magnitude of a will steadily approach that of c, i.e., the zone free of adhesive traction will grow more rapidly than the rate of increase of c and the annulus having the adhesive traction σ_{ad} will shrink. As the difference c–a shrinks, the relationship between the applied stress, σ_A, and the radius, a, of the traction free zone will approach the relationship between σ_A and a shown as the full line in Figure 4(a). We have shown a schematic for this situation as a dashed line in Figure 4(a), marked $\sigma_{ad}\langle\infty,\ \Delta_{ad}\rangle 0$.

The relationship shown as a dashed line for $\sigma_{ad}\langle\infty,\ \Delta_{ad}\rangle 0$ in Figure 4(a) and the remaining segment of the full line it merges with have an interesting feature. Starting with completely adhered half-spaces, we apply tensile stress, σ_A, and above a critical level a detachment of radius a will appear. However, the spreading of the detachment immediately becomes unstable, since the value of applied stress, σ_A, in equilibrium with the detachment radius, a, now begins to fall. If the applied stress can be reduced quickly enough, the propagation of the detachment can be arrested on the stable branch of the full line in Figure 4(a), in the region in which $b < a < a_m$. To extend the detachment further, the applied stress, σ_A, must be increased once more to σ_P, at which stage unstable pull-off will occur.

Thus, we have inferred that for realistic adhesive interactions such as the Dugdale model, there may be a bi-stable configuration of adhesion, as follows. A weak, stable, state of adhesion can be achieved with a finite zone of detachment present (i.e., with $b < a < a_m$) that can be pulled off relatively easily. If sufficient compression is applied to this state of adhesion of the half-spaces, they will jump together to adhere completely to each other. This state of adhesion is strong, with separation only possible by the application of a relatively high applied stress, as suggested in the schematic dashed line marked $\sigma_{ad}\langle\infty,\ \Delta_{ad}\rangle 0$ in Figure 4(a). Note that the transition between these two possible adhered states occurs in a non-equilibrium manner, and additional energy over and above the adhesion energy, w_0, will be dissipated or recovered in going back and forth between these states. Such additional dissipation, associated with possible adhesion hysteresis, has been addressed by Johnson,[7] Hui *et al.*,[8] and Guduru.[10]

Strong Adhesion, Compliant Materials, or a Shallow Dimple

Now consider adhesion between half-spaces having the interaction shown in Figure 4(b), i.e., $\delta_0^2 E^*/bw_0 < 2\pi$. This case is less interesting because there is no stable detachment of finite size at zero applied stress. Instead, for stable detachments, a finite applied stress must be applied, with pull-off occurring if it rises above the level σ_P. Similarly, if, for a stable detachment, the applied stress is relaxed below $\sqrt{\pi w_0 E^*/2b} - \delta_0 E^*/2b$ (i.e., the value of the equilibrium applied stress at $a = b$), the half-spaces will be drawn unstably into complete adhesion with a falling to zero. The model shows that an infinite applied stress is then required to pull the half-spaces apart again; as in the previous discussion, this feature is a limitation of the model and a van der Waals or Dugdale model of interaction between the surfaces would provide a finite separation strength. It should be noted that the feature in this case in which there is no stable, finite detachment size at zero applied load arises because the adhesion energy is sufficiently strong that it overcomes the elastic resistance to closure of any finite detachment.

Discussion

It has been shown that a dimple on the surface of an elastic half-space adhering to the boundary plane of another elastic half-space introduces interesting features into the phenomena of adhesion. When the adhesion is weak, the elastic materials involved are relatively stiff, and the dimple is sufficiently deep [i.e., as in Fig. 4(a)], bi-stable adhesion prevails. In the completely adhered state, a large applied stress is required to initiate detachment of the surfaces. This process will occur at first in a stable manner as the applied stress is increased, with the detachment radius gradually and stably becoming larger. At a critical level of the applied stress, the process becomes unstable, leading to complete detachment if the applied load is maintained. On the other hand, if the applied stress is reduced quickly to zero while this unstable detachment is occurring, the detachment radius can be arrested in a stable configuration. If the applied load is thereafter increased, stable extension of the detachment can be reinitiated. This process will continue until a second, lower, critical value of the applied stress is reached, whereupon unstable extension of the detachment will again commence, this time with the two half-spaces pulling away from each other to become completely detached.

These processes can be reversed, with adhesion being initiated by bringing the two surfaces into contact with each other to create a weakly adhered state with a finite region of detachment present. This weakly adhered state can be converted to a strongly adhered state by application of compression up to a critical level, whereupon the finite, detached segment at the interface will disappear. Thus, the system can be made to switch back and forth between a strongly adhered state and a weakly adhered condition. The weakly adhered state can be converted to the strongly adhered condition by the application of compression. Similarly, with careful control of the applied tension, the strongly adhered state can be converted to the weakly adhered condition.

These bi-stable states of adhesion controlled by the presence of a dimple may have practical significance, e.g., if it is desirable to instigate adhesion of the two bodies so that they can be readily pulled apart in some situations, but not in others. The usefulness of a one way system that can be

converted from the weak state to the strong state is obvious. It can be used in processes such as placement where a final, strong state of adhesion is undesirable until it is ascertained that the placing of the adhered component is correct. A disadvantage of the envisaged design of the paired surfaces is that the conversion from the strong state of adhesion to the weak one requires delicate application of tension to avoid unintentional separation of the surfaces. However, it is conceivable that the dimple shapes could be manipulated by, say, microfluidic channels in the underlying material[3] to reduce the depth of the dimples while the system is in its strongly adhered state. This step would make it easier to create a fresh detachment at the dimples, thereby reducing the tension necessary to convert the strong state of adhesion to the weak one.

Note also that paired surfaces with dimples of varying sizes spaced some distance apart would introduce progressive attachment and detachment in a reversible manner. This process would involve the shallowest dimples popping into intimate adhesive contact first at low levels of compression, with deeper ones adhering later as greater levels of compression are applied, until eventually all areas of detachment are eliminated at the highest level of compression. The adhered surfaces could then be detached from each other in a stable manner, with low tension causing the deepest dimples to switch first from intimate adhesion to a partially detached state, followed by the shallower ones doing so as the tension is increased. As the tension is increased, the detachments around the deeper dimples would then start to grow unstably, and the two surfaces would come apart.

Other phenomena might become important when the adhering surfaces have many dimples that are close together. It has been observed in experiments on fibrillar and patterned surfaces that adhesion is stronger than when the adhering surfaces are without fibrils or patterns, i.e., smooth and/or flat.[8–10,14–18] If the dominant phenomenon is the propagation of the detachment through the forest of closely-spaced, patterned features or fibrils, it is observed in the experiments that the front of the detachment becomes very irregular in shape. The greater adhesive strength for such surfaces can be rationalized as the effect of trapping of the detachment front in regions where the energy release rate at the detachment front is low due to its shape, perhaps also associated with regions of high adhesion energy caused by the complex patterning of the surface. We would expect the adhesion phenomena addressed in the current paper to be associated with widely separated dimples, with a transition to the trapping mode of detachment, along with enhancements to the dissipation of stored elastic energy, occurring for more closely spaced ones. Some insights on this point are available from the work of Johnson,[7] Hui *et al.*,[8] and Guduru[10] on the adhesion of periodically wavy surfaces.

Finally, we emphasize that the deductions drawn from our analysis do not depend on the special shape of dimple selected for our study (Fig. 1). This shape was chosen because the elasticity and fracture mechanics associated with the analysis of adhesion are essentially trivial, and do not require extensive numerical methods or partial differential equations. We believe that our results are representative of the effect of an arbitrary dimple, other than one having a nearly orthogonal intersection with the free surface.

Conclusions

A dimple on the surface of a half-space having an adhesive interaction with another half-space can introduce a stable state of adhesion between the half-spaces in which there is a finite region of detachment at zero applied load. This occurs when the materials are relatively stiff, the dimple is deep and the adhesion is relatively weak. When the materials are more compliant, the dimple is shallower and the adhesion is stronger, this stable state of adhesion with a detachment at the dimple at zero applied load does not occur. When the stable state of adhesion exists at zero applied load, with a detachment at the dimple, the surfaces can be pulled apart relatively easily by causing the detachment to propagate under tension. If compression is applied to the stable state of adhesion having a detachment present at the dimple at zero applied load, the detachment can be made to disappear completely, and a strong state of intimate adhesion is created. In such a state, the half-spaces will be more difficult to separate by application of applied load. Such bi-stable, switchable adhesion may have some practical utility in the development of adhesion systems.

Appendix I

Calculation of the Energy Release Rate, G: If $a \le b$, the stress at the interface prior to relaxation due to detachment is given by Equation (5a) everywhere on the surfaces of the detachment. If $a > b$, the interface stress within the detachment prior to relaxation is given by Equation (5a) where $r \le b$, and by Equation (5b) in the segment where $b < r \le a$. Consideration of fracture mechanics then gives us the Mode I stress intensity factor at the perimeter of the detachment as[13]

$$K_{\mathrm{I}} = \frac{2}{\pi}\left(\sigma_{\mathrm{A}} + \frac{\delta_0 E^*}{2b}\right)\sqrt{\pi a} \qquad a \le b \tag{I.1a}$$

$$K_{\mathrm{I}} = \frac{2}{\pi}\left[\sigma_{\mathrm{A}} + \frac{\delta_0 E^*}{2b}\left(1 - \sqrt{1 - \frac{b^2}{a^2}}\right)\right]\sqrt{\pi a} \qquad a > b \tag{I.1b}$$

Due to the lack of shear stress at the interface, the Mode II and Mode III stress intensity factors are zero. It then follows that the energy release rate, G, at the edge of the detachment is given by[7]

$$G = \frac{K_{\mathrm{I}}^2}{2E^*} \tag{I.2}$$

Thus

$$G = \frac{2aE^*}{\pi}\left(\frac{\sigma_{\mathrm{A}}}{E^*} + \frac{\delta_0}{2b}\right)^2 \qquad a \le b \tag{I.3a}$$

$$G = \frac{2aE^*}{\pi}\left[\frac{\sigma_A}{E^*} + \frac{\delta_0}{2b}\left(1 - \sqrt{1 - \frac{b^2}{a^2}}\right)\right]^2 \qquad a > b \tag{I.3b}$$

For equilibrium, the energy release rate must be equal to the adhesion energy, w_0. Replacement of G by w_0 in Equation (I.3) and rearrangement then gives the applied stress in equilibrium with a detachment of radius a. This result is stated in Equation (6).

Appendix II

Detachment Stability: Consider the stability of a detachment, i.e., its response to perturbations of its radius when the applied stress is held fixed. Stable equilibrium configurations are associated with a global or local minimum of the potential energy, $U(a, \sigma_A)$, of the system, with U consisting of contributions from the elastic, surface and interface energies, plus the potential energy of the applied load.[1] A standard result from fracture mechanics[19] provides us with

$$\frac{\partial U}{\partial a} = 2\pi a[w_0 - G] \tag{II.1}$$

Equilibrium is thus associated with the condition $\partial U/\partial a = 0$, giving rise to the requirement $G = w_0$ utilized above.[19] A consequence of Equation (II.1) is that a stable equilibrium state exists if $\partial G/\partial a < 0$. From Equation (I.3a) it is thus clear that the equilibrium configuration is unstable when $a < b$, a fact that is well-known from fracture mechanics.[20] Differentiation of Equation (I.3b) gives for $a > b$

$$\frac{\partial G}{\partial a} = \frac{2E^*}{\pi}\left[\frac{\sigma_A}{E^*} + \frac{\delta_0}{2b}\left(1 - \sqrt{1 - \frac{b^2}{a^2}}\right)\right] \times \left[\frac{\sigma_A}{E^*} + \frac{\delta_0}{2b}\left(1 - \sqrt{1 - \frac{b^2}{a^2}}\right) - \frac{\delta_0}{b}\frac{\frac{b^2}{a^2}}{\sqrt{1 - \frac{b^2}{a^2}}}\right] \tag{II.2}$$

Use of Equation (I.3b) again then provides

$$\left[\frac{\sigma_A}{E^*} + \frac{\delta_0}{2b}\left(1 - \sqrt{1 - \frac{b^2}{a^2}}\right)\right] = \sqrt{\frac{\pi G}{2aE^*}} \tag{II.3}$$

and substitution of this into Equation (II.2) leads to

$$\frac{\partial G}{\partial a} = \sqrt{\frac{8Ga}{\pi E^*}}\left(\sqrt{\frac{\pi G E^*}{8a^3}} - \frac{\delta_0 E^*}{2b}\frac{\frac{b^2}{a^3}}{\sqrt{1 - \frac{b^2}{a^2}}}\right) \tag{II.4}$$

The observation from Equation (6b) that in the equilibrium condition

$$\frac{\partial \sigma_A}{\partial a} = \frac{\delta_0 E^*}{2b}\frac{\frac{b^2}{a^3}}{\sqrt{1 - \frac{b^2}{a^2}}} - \sqrt{\frac{\pi w_0 E^*}{8a^3}} \tag{II.5}$$

and that $G = w_0$ allows Equation (II.4) to be converted to

$$\frac{\partial G}{\partial a} = -\sqrt{\frac{8w_0 a}{\pi E*}}\frac{\partial \sigma_A}{\partial a} \tag{II.6}$$

Since the square root term is positive, this equation demonstrates that in the equilibrium configuration the gradient of the energy release rate with respect to the radius of the detachment has a sign opposite to that of the gradient of the applied stress. Thus, stability of the equilibrium configuration is assured if $\partial \sigma_A/\partial a > 0$, where σ_A is the applied stress in equilibrium with a detachment of radius a as given by Equation (6).

Appendix III

Stability of Detachment Growth in a Cohesive Zone (Dugdale) Model: The question of stability of detachment growth will be addressed only at the stage where the traction free detachment appears whilst fully adhered surfaces are being pulled apart by a tensile applied load. At lower levels of the applied load, the interaction of the surfaces is encompassed by the cohesive interaction where there is a separation of the surfaces. When the critical separation, Δ_{ad}, is reached, a traction free separation will appear and grow in length. We are interested in whether the growth of this zone occurs under a rising applied load or if it involves the reduction of the load and, therefore, instability of the process. Ideally, we should do this by addressing the axisymmetric problem presented by our dimple. However, the relevant results are not available in a simple form, making numerical computations necessary. Instead, we analyze the plane strain situation and infer our assessment from that.

The plane strain problem can be undertaken with reference to Figures 1–3. However, now the shape of the upper surface in Figure 1 is given by[21]

$$\delta(x) - \delta(b) = \frac{\delta_0 x}{b \ln 4}\ln\frac{b - x}{b + x} - \frac{\delta_0}{\ln 4}\ln\frac{b^2 - x^2}{4b^2} \qquad \frac{x}{b} \le 1 \tag{III.1a}$$

$$\delta(x) - \delta(b) = \frac{\delta_0 x}{b \ln 4}\ln\frac{x - b}{x + b} - \frac{\delta_0}{\ln 4}\ln\frac{x^2 - b^2}{4b^2} \qquad \frac{x}{b} \ge 1 \tag{III.1b}$$

where x has been used instead of the parameter r of the figure to emphasize the plane nature of the problem being addressed. Note that this shape suffers from the usual difficulty of divergence at infinity associated with half space problems in planar analysis; this feature will not cloud the insights we obtain. When the two surfaces are fully adhered to each other as in Figure 2, but without applied load, the tensile traction on the interface between them is given by

$$T = \frac{\pi E^* \delta_0}{b \ln 4} \qquad \frac{x}{b} \le 1 \tag{III.2}$$

and zero elsewhere. Therefore, when a stress, σ_A, is applied, as in Figure 2, the traction across the interface, when the surfaces

are fully adhered with no gap between them, is

$$\sigma_{zz} = \sigma_A + \frac{\pi E^* \delta_0}{b \ln 4} \qquad \frac{x}{b} \le 1 \tag{III.3a}$$

$$\sigma_{zz} = \sigma_A \qquad \frac{x}{b} \ge 1 \tag{III.3b}$$

Therefore, Equation (III.3a) replaces the notation on Figure 2 regarding the stress or traction at the interface between $-b$ and b.

When σ_{zz} at the interface reaches the adhesive strength, σ_{ad}, a gap, $\Delta(x)$, will appear between the surfaces, extending out to the location $|x| = c \ge b$. As long as $\Delta(x) \le \Delta_{ad}$ everywhere, the parameter c is obtained in the usual way by considering there to be a crack extending to length $2c$ and setting its stress intensity factor[13]

$$K_I = \left[(\sigma_A - \sigma_{ad}) + \frac{2E^* \delta_0}{b \ln 4}\left(\sin^{-1}\frac{b}{c}\right)\right]\sqrt{\pi c} \tag{III.4}$$

to zero, giving

$$c = b \csc\left[\frac{(\sigma_{ad} - \sigma_A) b \ln 4}{2E^* \delta_0}\right] \tag{III.5}$$

In this circumstance, the gap at $x = 0$ is[13]

$$\Delta(0) = \frac{4\delta_0}{\ln 4} \coth^{-1}\left\{\sec\left[\frac{(\sigma_{ad} - \sigma_A) b \ln 4}{2E^* \delta_0}\right]\right\} \tag{III.6}$$

and elsewhere the gap is smaller.

The results in the previous paragraph are valid until $\Delta(0) = \Delta_{ad}$, at which stage a traction free section of detachment will begin to appear at $x = 0$, since the two surfaces will there be moving away from each other beyond the interaction limit, Δ_{ad}. The applied stress at which the traction free detachment will appear is thus given by

$$\sigma_A = \sigma_{ad} - \frac{2E^* \delta_0}{b \ln 4} \cos^{-1}\left[\frac{1}{\coth\left(\frac{\Delta_{ad} \ln 4}{4\delta_0}\right)}\right] \tag{III.7}$$

and the results in the previous paragraph are valid for values below this level. Note that as Δ_{ad} approaches zero, and therefore as Δ_{ad} becomes very large, the value of the applied stress at which the traction free detachment appears is, to first order,

$$\sigma_A = \sigma_{ad} - \frac{\pi E^* \delta_0}{b \ln 4} + \frac{E^* \Delta_{ad}}{2b} \tag{III.8}$$

so that $\sigma_A + T$ lies above σ_{ad} by a very small fraction of E^*. The corresponding value of c is given to first order by

$$c = b\left[1 + \frac{1}{2}\left(\frac{\Delta_{ad} \ln 4}{4\delta_0}\right)^2\right] \tag{III.9}$$

For values of applied stress higher than that given in Equation (III.7), a traction free detachment of length $2a$ is present and is symmetric about the origin. The relationship among the applied stress, c and a is obtained by calculating the stress intensity factor for a crack of length $2c$,[13]

$$K_I = \left[(\sigma_A - \sigma_{ad}) + \frac{2E^* \delta_0}{b \ln 4}\left(\sin^{-1}\frac{b}{c}\right) + \frac{2\sigma_{ad}}{\pi}\left(\sin^{-1}\frac{a}{c}\right)\right]\sqrt{\pi c} \tag{III.10}$$

and setting it to zero, thereby requiring the term in the brackets in Equation (III.10) to disappear. The gap at $x = a$ for the case $a < b$ is then given by[13]

$$\Delta(a) = \frac{4\delta_0}{\ln 4}\left\{\coth^{-1}\left[\sqrt{\frac{1-(a/c)^2}{1-(b/c)^2}}\right] - \frac{a}{b}\coth^{-1}\left[\sqrt{\frac{(c/a)^2-1}{(c/b)^2-1}}\right]\right\} + \frac{4\sigma_{ad} a}{\pi E^*} \ln\frac{c}{a} \tag{III.11}$$

and the cohesive zone law requires this to be equal to Δ_{ad}, furnishing a condition that must be satisfied by a and c. It follows that, together, Equation (III.10), with $K_I = 0$ and Equation (III.11), with $\Delta(a) = \Delta_{ad}$, provide the equations from which the dependence of σ_A on a can be obtained. We are interested in the value of $d\sigma_A/da$ when $a = 0$ to determine whether it is positive (stability with a rising applied stress) or negative (instability with a falling applied stress). Therefore, we should differentiate Equation (III.10) and (III.11) with respect to σ_A, c, and a, subject to $K_I = 0$ and $\Delta(a) = \Delta_{ad}$, and then solve the resulting simultaneous equations for $d\sigma_A/da$, with $a = 0$. Such a procedure produces

$$d\sigma_A = -\frac{2E^* \delta_0}{b \ln 4} \frac{1}{\sqrt{1-(b/c)^2}} d\left(\frac{b}{c}\right) - \frac{2\sigma_{ad}}{\pi} \times \frac{1}{\sqrt{1-(a/c)^2}} d\left(\frac{a}{c}\right) \tag{III.12}$$

and

$$\frac{\sigma_{ad} b \ln 4}{\pi E^* \delta_0}\left\{d\left[\frac{a}{c}\ln\left(\frac{c}{a}\right)\right] - \frac{a}{b}\ln\left(\frac{c}{a}\right) d\left(\frac{b}{c}\right)\right\} - \sqrt{\frac{1-(a/c)^2}{1-(b/c)^2}} d\left(\frac{b}{c}\right) - \coth^{-1}\left[\sqrt{\frac{(c/a)^2-1}{(c/b)^2-1}}\right] \times \left[d\left(\frac{a}{c}\right) - \frac{a}{b} d\left(\frac{b}{c}\right)\right] = 0 \tag{III.13}$$

In the limit as a goes to zero, the dominant terms from Equation (III.13) balance according to

$$\frac{1}{\sqrt{1-(b/c)^2}} d\left(\frac{b}{c}\right) = \frac{\sigma_{ad} b \ln 4}{\pi E^* \delta_0} d\left[\frac{a}{c}\ln\left(\frac{c}{a}\right)\right] \tag{III.14}$$

and then Equation (III.12) gives us

$$\lim_{x\to 0} \frac{d\sigma_A}{da} = -\lim_{x\to 0} \frac{2\sigma_{ad}}{\pi c} \ln\left(\frac{c}{a}\right) = -\infty \tag{III.15}$$

demonstrating that the applied stress immediately falls rapidly as the detached zone with zero traction appears and grows to finite length. As noted above in connection with Equation (III.8), when Δ_{ad} is very small, this event will take place when σ_A lies above $\sigma_{ad} - T$ by a small amount. From these results, we infer that a similar behavior will occur for an axisymmetric

ADVANCED ENGINEERING MATERIALS

dimple, and represent this with a dashed line marked $\sigma_{ad}\langle\infty,\ \Delta_{ad}\rangle 0 \in$ in Figure (4a).

Received: February 23, 2010
Final Version: February 25, 2010

[1] J. N. Israelachvili, *Intermolecular and Surface Forces*, Academic Press, **1991**.
[2] M. Kamperman, E. Kroner, A. del Campo, R. McMeeking, E. Arzt, *Adv. Eng. Mater.* **2010**, this issue.
[3] A. Majumdar, A. Ghatak, A. Sharma, *Science* **2007**, *318*, 258.
[4] K. L. Johnson, K. Kendall, A. D. Roberts, *Proc. R. Soc. Lond, A* **1971**, *324*, 301.
[5] D. Maugis, *J. Colloid Interface Sci.* **1992**, *150*, 243.
[6] K. S. Kim, R. M. McMeeking, K. L. Johnson, *J. Mech. Phys. Solids* **1998**, *46*, 243.
[7] K. L. Johnson, *Int. J. Solids Struct.* **1985**, *32*, 423.
[8] C. Y. Hui, Y. Y. Lin, J. M. Baney, E. J. Kramer, *J. Polym. Sci. B* **2001**, *39*, 1196.
[9] G. Carbone, L. Mangialardi, *J. Mech. Phys. Solids* **2004**, *52*, 1267.
[10] P. R. Guduru, *J. Mech. Phys. Solids* **2007**, *55*, 445.
[11] K. L. Johnson, *Contact Mechanics*, Cambridge University Press, **1985**.
[12] H. Gao, H. Yao, *PNAS* **2004**, *101*, 7851.
[13] H. Tada, P. C. Paris, G. R. Irwin, *The Stress Analysis of Cracks Handbook*, Del Research Corporation, St. Louis **1985**.
[14] A. Ghatak, L. Mahadevan, J. Y. Chung, M. K. Chaudhury, V. Shenoy, *Proc. R. Soc. Lond, A* **2004**, *460*, 2725.
[15] C.-Y. Hui, N. J. Glassmaker, T. Tang, A. Jagota, *J. R. Soc. Interface* **2004**, *1*, 35.
[16] N. J. Glassmaker, A. Jagota, C.-Y. Hui, *Acta Biomater.* **2005**, *1*, 367.
[17] A. J. Crosby, M. Hageman, A. Duncan, *Langmuir* **2005**, *21*, 11738.
[18] C. Greiner, A. del Campo, E. Arzt, *Langmuir* **2007**, *23*, 3495.
[19] A. A. Griffith, *Philos. Trans. R. Soc. Lond.* **1920**, *221*, 163.
[20] T. L. Anderson, *Fracture Mechanics Fundamentals and Applications*, 2nd Edn. CRC Press, **1995**.
[21] S. Timoshenko, J. N. Goodier, *Theory of Elasticity*, McGraw-Hill **1960**.

